Vol 17 No 7, July 2008
1674-1056/2008/17(07)/2458-08

Chinese Physics B

© 2008 Chin. Phys. Soc.
and IOP Publishing Ltd

Transverse momentum and transverse mass distributions of charged hadrons produced in Au–Au collisions at high energies*

Liu Fu-Hu(刘福虎)†

Institute of Theoretical Physics, Shanxi University, Taiyuan 030006, *China*

(Received 14 October 2007; revised manuscript received 7 November 2007)

The transverse momentum distribution and the transverse mass distribution of charged hadrons produced in nucleus–nucleus collisions at high energies are described by using a two-cylinder model. The results calculated by the model are compared and found to be in agreement with the experimental data of the STAR and E895 Collaborations, measured in Au–Au collisions at the relativistic heavy ion collider (RHIC) and alternating-gradient synchrotron (AGS) energies, respectively. In the energy range concerned, the excitation degree of emission source close to the central axis of cylinders increases obviously with the collision centrality and incident energy increasing, but it does not show any obvious change with the increase of the (pseudo)rapidity in central collisions. The excitation degree of emission source close to the side-surface of cylinders does not show any obvious change with the collision centrality, the (pseudo)rapidity, and the incident energy increasing.

Keywords: transverse momentum, two-cylinder model, nucleus–nucleus collisions
PACC: 2500, 2570, 1440D, 1440F

1. Introduction

In nucleus–nucleus collisions at high energies,[1−5] many particles and fragments are emitted.[6−10] The majority of particles emitted from such collisions are pions.[11−15] The measured pion and other hadron distributions retain information about the production process and allow the amount of energy available for particle production to be determined.[16]

In the past 20–30 years, many theoretical and experimental studies have been carried out. Different phenomenological mechanisms of initial coherent multiple interactions and particle transport were proposed.[17−19] According to the fireball model[20] and the string model,[21] we suggested a thermalized cylinder model[22−25] and developed the model into a two-cylinder model.[26−28] It is known that the two-cylinder model is successful in describing (pseudo)rapidity distributions of charged particles produced in nucleus–nucleus collisions in an energy range from 400A MeV to 100A TeV,[29] where A denotes the nucleon number in a nucleus, 1MeV = 10^6eV (electron volt), and 1TeV = 10^{12}eV. In the description of transverse momentum and transverse mass distributions of charged particles, the model needs developing and testing.

In this paper, we will use and develop the two-cylinder model to describe the transverse momentum and transverse mass distributions of charged pions and other hadrons produced in nucleus–nucleus collisions at high energies and compare our calculated results with the experimental data of the STAR and E895 Collaborations, measured in Au–Au collisions at the relativistic heavy ion collider (RHIC) and alternating-gradient synchrotron (AGS) energies, respectively. In Section 2, the two-cylinder model is described. A comparison between calculated results and experimental data is shown in Section 3. Finally, discussion and conclusions are given in Section 4.

2. The model

According to the two-cylinder model,[26−28] we assume that a projectile cylinder and a target cylinder are formed in nucleus–nucleus collisions at intermediate, high, or ultra-high energies. At intermediate ener-

*Project supported by the National Natural Science Foundation of China (Grant Nos 10675077 and 10275042), the Shanxi Provincial Natural Science Foundation of China (Grant No 2007011005), and the Shanxi Provincial Foundation of China for Returned Overseas Scholars.
†E-mail: fuhuliu@163.com

gies, the two cylinders overlap each other totally, and the interacting system, in fact, may be described by a single cylinder model. At high energies, the two cylinders overlap each other partly. At ultra-high energies, there is a gap appearing between the two cylinders.

In the rapidity space, the projectile cylinder and target cylinder are assumed to lie in the rapidity ranges $[y_{\mathrm{P\,min}}, y_{\mathrm{P\,max}}]$ and $[y_{\mathrm{T\,min}}, y_{\mathrm{T\,max}}]$ respectively.[26−28] The centre rapidity of the interacting system is denoted by y_{C} (or y_{cm}). Let Δy denote the rapidity shift of the projectile and target cylinder centres, and let Dy denote that of the leading projectile and target protons, from the centre-of-mass of collisions. The lengths of the two cylinders are the same, and can be defined as $2\delta y \equiv (y_{\mathrm{P\,max}} - y_{\mathrm{P\,min}}) = (y_{\mathrm{T\,max}} - y_{\mathrm{T\,min}})$. Using the parameters Δy, δy, and Dy, as well as the contributions of leading protons, we can describe pseudorapidity distributions of charged particles produced in nucleus–nucleus collisions in an energy range from $400A$ MeV to $100A$ TeV.[29]

In the description of transverse momentum and transverse mass distributions, we need to use the excitation degree of emission source. Along the beam direction, the emission points with the same rapidity in the cylinder cut region form an emission plane in the rapidity space. In the same emission plane, the excitation degree decreases along the transverse direction. The emission points with the same excitation degree in the same emission plane form an emission circle in the transverse momentum space. In the two cylinders, the emission circles with the same excitation degree form an emission source. The emission source is in fact the side-surface of a subcylinder, where the subcylinder is a cylinder shaped iso-'excitation-degree' surface. This would correspond to an iso-potential surface in ordinary electromagnetism language. The excitation degree of emission source close to the central axis is greater than that of emission source close to the side-surface of the two cylinders.

Let the beam be directed along the oz axis and the reaction plane lie in the xoz plane. In an emission source concerned, in the different rest frames of different emission circles, we assume that the three momentum components p_x^*, p_y^*, and p_z^* obey the Gaussian distributions having the same width σ. On the central axis and the side-surface of two cylinders, the momentum distribution widths are denoted by σ_{c} and σ_{s} respectively. From central axis to side-surface, the contribution of emission source is assumed to increase linearly with σ decreasing. It is easy to know that the transverse momentum $p_{\mathrm{T}}^* = \sqrt{p_x^{*2} + p_y^{*2}} = p_{\mathrm{T}}$, which has the same distribution form in different reference frames, obeys the Rayleigh distribution

$$\begin{aligned} f(p_{\mathrm{T}}^*) =& \frac{p_{\mathrm{T}}^*}{\sigma^2}\exp\left(-\frac{p_{\mathrm{T}}^{*2}}{2\sigma^2}\right) \\ =& \frac{p_{\mathrm{T}}}{\sigma^2}\exp\left(-\frac{p_{\mathrm{T}}^2}{2\sigma^2}\right) = f(p_{\mathrm{T}}). \end{aligned} \tag{1}$$

The above distribution describes the transverse momentum distribution of particles produced in the side-surface of sub-cylinder with a given excitation degree. The transverse momentum distribution of particles produced in the two cylinders is the sum of contributions of all sub-cylinders. We have

$$\begin{aligned} f_{\mathrm{P_T}}(p_{\mathrm{T}}) =& C\int_{\sigma_{\mathrm{s}}}^{\sigma_{\mathrm{c}}} (\sigma_{\mathrm{c}} - \sigma) f(p_{\mathrm{T}})\mathrm{d}\sigma \\ =& C\int_{\sigma_{\mathrm{s}}}^{\sigma_{\mathrm{c}}} (\sigma_{\mathrm{c}} - \sigma)\frac{p_{\mathrm{T}}}{\sigma^2} \\ & \times \exp\left(-\frac{p_{\mathrm{T}}^2}{2\sigma^2}\right)\mathrm{d}\sigma, \end{aligned} \tag{2}$$

where C is the normalization constant. Similarly, the distribution of transverse mass $m_{\mathrm{T}} = \sqrt{p_{\mathrm{T}}^2 + m_0^2}$ is given by

$$\begin{aligned} f_{m_{\mathrm{T}}}(m_{\mathrm{T}}) =& C\int_{\sigma_{\mathrm{s}}}^{\sigma_{\mathrm{c}}} (\sigma_{\mathrm{c}} - \sigma)\frac{m_{\mathrm{T}}}{\sigma^2} \\ & \times \exp\left(-\frac{m_{\mathrm{T}}^2 - m_0^2}{2\sigma^2}\right)\mathrm{d}\sigma, \end{aligned} \tag{3}$$

where m_0 is the rest mass of a relevant particle. For a given particle, for example for a pion, we use m_π instead of m_0.

In the above discussion, there are two free parameters σ_{s} and σ_{c} involved in the calculations of transverse momentum and transverse mass distributions. The values of σ_{s} and σ_{c} indicated the momentum distribution widths of particles produced on the side-surface and the central axis of two cylinders respectively. The excitation degree of emission source can be described by σ_{s} or σ_{c}. A greater σ (σ_{s} or σ_{c}) corresponds to a higher degree of excitation.

3. Comparison between calculations and measurements

The transverse momentum distributions, $(1/p_{\mathrm{T}})\mathrm{d}^2N/\mathrm{d}p_{\mathrm{T}}\mathrm{d}\eta$, of positively and negatively charged hadrons produced in Au–Au collisions at

the centre-of-mass energy $\sqrt{s}$=130A GeV (the RHIC energy, 1 GeV = 10^9 eV), for nine classes of multiplicity (centrality) in the pseudorapidity interval $|\eta| < 0.5$, are presented in Figs.1 and 2 respectively. The circles denote the experimental data of the STAR Collaboration[30] and the curves represent our calculated results from expression (2). From 0–5% to 70–80%, the spectra are scaled by successive powers

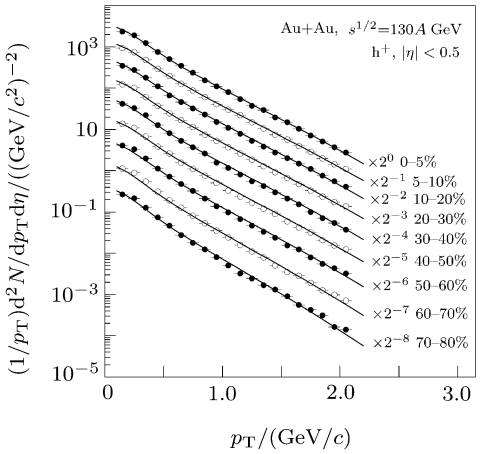


Fig.1. Transverse momentum distributions, $(1/p_T)d^2N/dp_Td\eta$, of positively charged hadrons produced in Au–Au collisions at $\sqrt{s}$=130A GeV for nine classes of multiplicity (centrality) in the pseudorapidity interval $|\eta| < 0.5$. The circles denote the experimental data of the STAR Collaboration[30] and the curves represent our calculated results. From 0–5% to 70–80%, the spectra are scaled by successive powers of 2 as indicated.

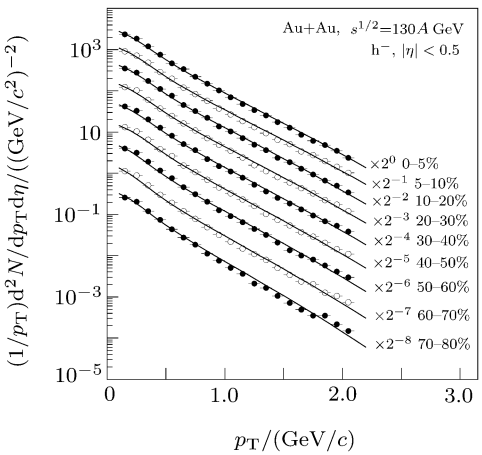


Fig.2. The caption is the same as that for Fig.1, but showing distributions of negatively charged hadrons.

of 2 as indicated. The values of σ_s and σ_c obtained by fitting the experimental data are shown in Table 1, where c in GeV/c in the table denotes the velocity of light in a vacuum. In the selection of parameter values, the method of χ^2-testing is used. One can see that expression (2) describes the transverse momentum distributions of charged hadrons produced in Au–Au collisions at the RHIC energies in the pseudorapidity interval $|\eta| < 0.5$. The values of σ_s do not change obviously and the values of σ_c increase with multiplicity (centrality) increasing.

Table 1. Parameter values of $\sigma_s - \sigma_c$ in GeV/c for curves in Figs.1–4.

Centrality	Fig.1	Fig.2	Fig.3	Fig.4
0–5%	0.15–0.98	0.15–0.98	0.11–0.86	0.11–0.86
5–10%	0.15–0.98	0.15–0.98	0.11–0.84	0.11–0.84
10–20%	0.15–0.98	0.15–0.96	0.11–0.85	0.10–0.85
20–30%	0.15–0.97	0.15–0.96	0.11–0.84	0.10–0.83
30–40%	0.15–0.96	0.15–0.95	0.10–0.83	0.10–0.83
40–50%	0.15–0.95	0.15–0.93	0.10–0.82	0.10–0.82
50–60%	0.15–0.93	0.14–0.92	0.09–0.78	0.09–0.78
60–70%	0.14–0.90	0.13–0.90	0.09–0.74	0.09–0.72
70–80%	0.14–0.86	0.14–0.87	0.09–0.70	0.09–0.70

The transverse momentum distributions, $(1/p_T)d^2N/dp_Tdy$, of positively and negatively charged pions produced in Au–Au collisions at $\sqrt{s}$=130A GeV, for nine classes of multiplicity (centrality) in the rapidity interval $|y| < 0.5$, are shown in Figs.3 and 4 respectively. The circles denote the experimental data of the STAR Collaboration[30] and

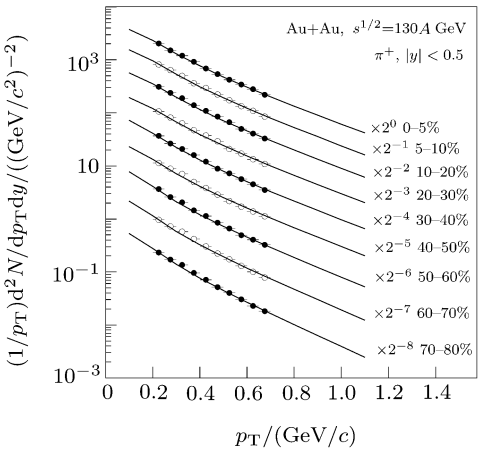


Fig.3. Transverse momentum distributions, $(1/p_T)d^2N/dp_Tdy$, of positively charged pions produced in Au–Au collisions at $\sqrt{s}$=130A GeV for nine classes of multiplicity (centrality) in the rapidity interval $|y| < 0.5$. The circles denote the experimental data of the STAR Collaboration[30] and the curves represent our calculated results. From 0–5% to 70–80%, the spectra are scaled by successive powers of 2 as indicated.

the curves represent our calculated results from expression (2). From 0–5% to 70–80%, the spectra are scaled by successive powers of 2 as indicated. The

values of σ_s and σ_c obtained by fitting the experimental data are shown in Table 1. The same conclusion from Figs.3 and 4 as from Figs.1 and 2 can be obtained. Expression (2) describes the transverse momentum distributions of charged pions produced in Au–Au collisions at the RHIC energy in the rapidity interval $|y| < 0.5$. The values of σ_s do not change obviously but the values of σ_c increase with multiplicity (centrality) increasing.

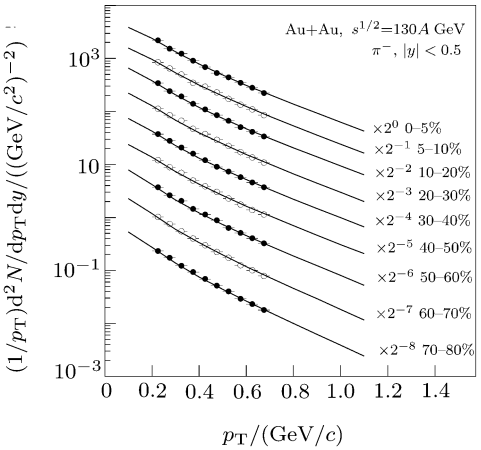


Fig.4. The caption is the same as that for Fig.3, but showing distributions of negatively charged pions.

In Figs.5 and 6, the transverse momentum distributions, $(1/p_T)d^2N/dp_Td\eta$, of positively and negatively charged hadrons produced in Au–Au collisions at $\sqrt{s}$=130A GeV, for twenty classes of pseudorapidity in the 5% most central events, are given respectively. The circles denote the experimental data of the STAR

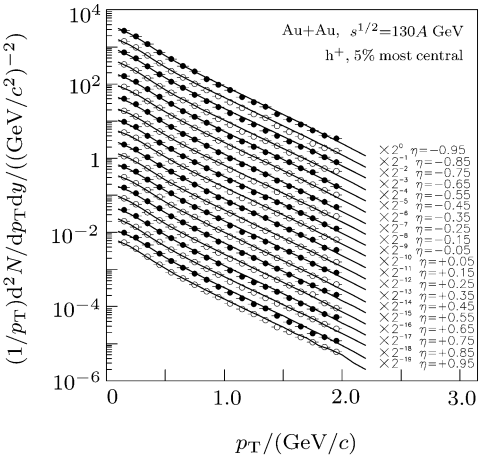


Fig.5. Transverse momentum distributions, $(1/p_T)d^2N/dp_Td\eta$, of positively charged hadrons produced in Au–Au collisions at $\sqrt{s}$=130A GeV for twenty classes of pseudorapidity classes in the 5% most central events. The circles denote the experimental data of the STAR Collaboration[30] and the curves represent our calculated results. From $\eta = -0.95$ to $\eta = 0.95$, the spectra are scaled by successive powers of 2 as indicated.

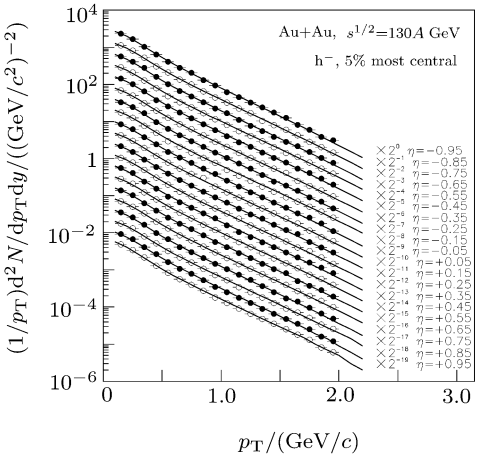


Fig.6. The caption is the same as that for Fig.6, but showing distributions of negatively charged hadrons.

Collaboration[30] and the curves represent our calculated results from expression (2). From $\eta = -0.95$ to $\eta = 0.95$, the spectra are scaled by successive powers of 2 as indicated. The values of σ_s and σ_c obtained by fitting the experimental data are shown in Table 2. In the selection of parameter values, the method of χ^2-testing is used. One can see that expression (2) describes the transverse momentum distributions of charged hadrons produced in Au–Au collisions at the RHIC energy in the 5% most central events. The values of σ_s and σ_c do not change obviously with pseudorapidity increasing.

Table 2. Parameter values of $\sigma_s - \sigma_c$ in GeV/c for curves in Figs.5–8.

η or y	Fig. 5	Fig. 6	Fig. 7	Fig. 8
−0.95	0.14–0.95	0.15–0.95	0.11–0.86	0.10–0.86
−0.85	0.14–0.95	0.15–0.96	0.11–0.86	0.11–0.86
−0.75	0.14–0.95	0.15–0.96	0.11–0.86	0.11–0.86
−0.65	0.14–0.95	0.15–0.97	0.11–0.86	0.11–0.86
−0.55	0.15–0.95	0.15–0.97	0.11–0.86	0.11–0.86
−0.45	0.15–0.95	0.15–0.97	0.11–0.85	0.11–0.85
−0.35	0.15–0.95	0.15–0.97	0.11–0.86	0.11–0.86
−0.25	0.15–0.96	0.15–0.98	0.10–0.82	0.10–0.82
−0.15	0.15–0.96	0.15–0.97	0.11–0.85	0.11–0.85
−0.05	0.15–0.96	0.15–0.97	0.10–0.85	0.10–0.85
0.05	0.15–0.96	0.15–0.97	0.10–0.85	0.10–0.85
0.15	0.15–0.96	0.15–0.97	0.10–0.85	0.10–0.85
0.25	0.15–0.96	0.15–0.97	0.09–0.82	0.09–0.83
0.35	0.15–0.95	0.15–0.97	0.10–0.81	0.11–0.82
0.45	0.15–0.95	0.15–0.97	0.11–0.85	0.11–0.85
0.55	0.14–0.95	0.15–0.97	0.10–0.84	0.10–0.84
0.65	0.15–0.95	0.15–0.96	0.11–0.86	0.11–0.86
0.75	0.14–0.96	0.15–0.97	0.10–0.86	0.10–0.86
0.85	0.15–0.95	0.15–0.96	0.10–0.86	0.10–0.86
0.95	0.14–0.95	0.14–0.97	0.09–0.81	0.09–0.81

In Figs.7 and 8, the transverse momentum distributions, $(1/p_{\rm T}){\rm d}^2N/{\rm d}p_{\rm T}{\rm d}y$, of positively and negatively charged pions produced in Au–Au collisions at $\sqrt{s}$=130A GeV, for twenty classes of rapidity in the 5% most central events, are given respectively. The circles denote the experimental data of the STAR Collaboration[30] and the curves represent our calculated results from expression (2). From $y=-0.95$ to $y=0.95$, the spectra are scaled by successive powers of 2 as indicated. The values of $\sigma_{\rm s}$ and $\sigma_{\rm c}$ obtained by fitting the experimental data are shown in Table 2. The same conclusion from Figs.7 and 8 as from Figs.5 and 6 can be obtained. Expression (2) describes the transverse momentum distributions of charged pions produced in Au–Au collisions at the RHIC energy in the 5% most central events. The values of $\sigma_{\rm s}$ and $\sigma_{\rm c}$ do not change obviously with rapidity increasing.

The transverse mass distributions, $(1/2\pi m_{\rm T}){\rm d}^2N/{\rm d}m_{\rm T}{\rm d}y$, of positively and negatively charged pions produced in Au–Au collisions at the AGS energies, in the rapidity interval $|y-y_{\rm cm}|<0.05$, are given in Figs.9 and 10 respectively. The circles denote the experimental data of the E895 Collaboration[31] and the curves represent our calculated results from expression (3). From 2A to 8A GeV, the spectra are scaled by successive powers of 10 as indicated. In Fig.9, for incident energies 2A, 4A, 6A, and 8A GeV,

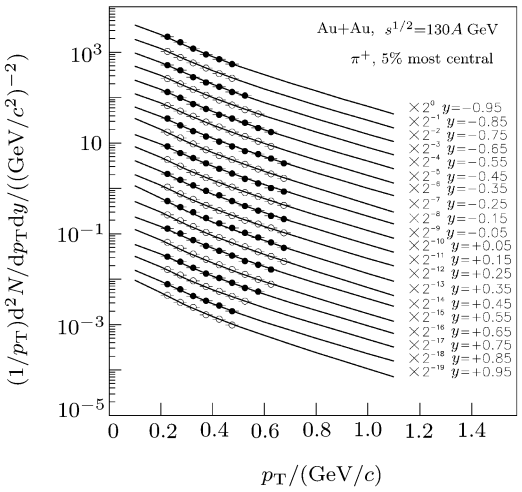


Fig.7. Transverse momentum distributions, $(1/p_{\rm T}){\rm d}^2N/{\rm d}p_{\rm T}{\rm d}y$, of positively charged pions produced in Au–Au collisions at $\sqrt{s}$=130A GeV for twenty classes of rapidity in the 5% most central events. The circles denote the experimental data of the STAR Collaboration[30] and the curves represent our calculated results. From $y=-0.95$ to $y=0.95$, the spectra are scaled by successive powers of 2 as indicated.

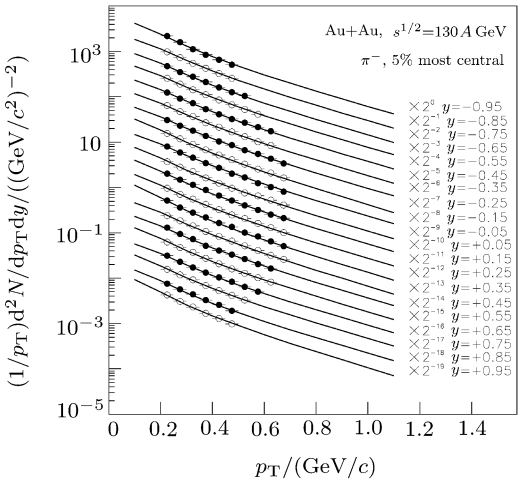


Fig.8. The caption is the same as for that Fig.7, but showing distributions of negatively charged pions.

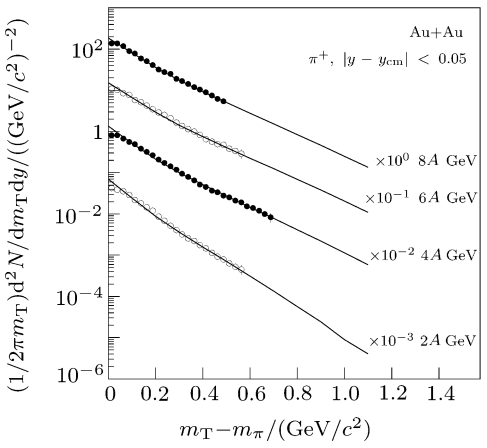


Fig.9. Transverse mass distributions, $(1/2\pi m_{\rm T}){\rm d}^2N/{\rm d}m_{\rm T}{\rm d}y$, of positively charged pions produced in Au–Au collisions at the AGS energies in the rapidity interval $|y-y_{\rm cm}|<0.05$. The circles denote the experimental data of the E895 Collaboration[31] and the curves represent our calculated results. From 2A to 8A GeV, the spectra are scaled by successive powers of 10 as indicated.

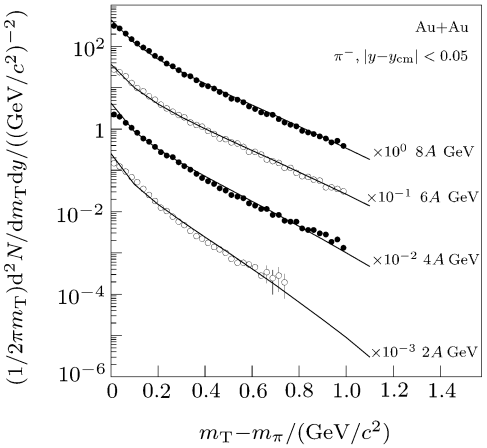


Fig.10. The caption is the same as that for Fig.9, but showing distributions of negatively charged pions.

the values of parameters in the form of $\sigma_s - \sigma_c$ obtained by fitting the experimental data are 0.09–0.42, 0.09–0.54, 0.10–0.57, and 0.10–0.57GeV/c, respectively. In Fig.10, the parameter values are 0.06–0.39, 0.06–0.49, 0.07–0.56, and 0.07–0.57GeV/c, respectively. In the selection of parameter values, the method of χ^2-testing is used. One can see that expression (3) describes the transverse mass distributions of charged pions produced in Au–Au collisions at the AGS energies in the rapidity interval $|y - y_{cm}| < 0.05$. The values of σ_s do not show an obvious change from $2A$ to $8A$ GeV, and the values of σ_c increase with incident energy increasing.

In above comparison, the experimental data are fitted to the extract parameters σ_s and σ_c. We present two large tables with very similar (but not exactly the same) values of these parameters. In some cases, the results for positive and negative particles differ from each other at the same centrality and (pseudo)rapidity. We believe that the statistical fluctuation would be responsible for the difference in parameter value between positive and negative particles. In Figs.1–8, we have analysed the experimental data of the STAR Collaboration.[31] The experimental data are similar in some cases. This leads the figures to be similar, too.

The experimental data are obtained to be 7–10 decades in number. It is difficult to see how good the fits are in figures. To see the quality of the fits, we have calculated the values of χ^2/degree of freedom (dof) for all fits. It is shown that the maximum value of χ^2/dof is 1.26 corresponding to the last fit in Fig.10, and the minimum value of χ^2/dof is 0.21 corresponding to the second fit in Fig.7.

4. Discussion and conclusions

The term 'excitation degree' has been used several times above. The excitation degree may be understood to be the value of σ_s or σ_c. A greater value of σ (σ_s or σ_c) corresponds to a higher degree of excitation. As indicated by a Boltzmann distribution, the 'temperature' of emission source seems to be able to be given by σ^2/m, where m is the mass of a particle concerned. According to Tables 1 and 2, the 'temperatures' in the side-surface region of cylinders are estimated to be in a range of 60–90MeV. The 'temperatures' of the central axis region of cylinders in central collisions are estimated to be in a range of 4700–5200MeV, and the 'temperature' in peripheral collisions is estimated to be 3500 MeV. If we consider the maximum Lorentz factor (~ 1.5) in the rapidity interval concerned, the three 'temperatures' are estimated to be in ranges of 40–60MeV, 3100–3500MeV, and 2300MeV, respectively.

One can see that the estimated 'temperature' in the central axis region is too high. It should be pointed out that what we do for expressions (2) and (3) is only fitting to the transverse momentum and the transverse mass. As this is not based on a thermodynamic equilibrium or a local thermodynamic equilibrium, the corresponding inverse slope used in the present work cannot be called temperature in the conventional sense. Therefore it cannot be compared directly with the temperature obtained from others. We would rather regard the inverse slope used in the present work as a common parameter.

In summary, the transverse momentum and transverse mass distributions of charged hadrons produced in Au–Au collisions at the RHIC and AGS energies have been studied by the two-cylinder model; a simple formula which describes the transverse momentum distributions is obtained; with the relationship between the transverse momentum and transverse mass considered, another formula which describes the transverse mass distributions is obtained; the two formulas have the same free parameters; the model is shown to be successful in describing of charged hadron transverse momentum and transverse mass distributions at the energy range concerned.

In addition, the parameters σ_s and σ_c describe the excitation degrees of emission sources close to the side-surface and the central axis of cylinders respectively. The values of σ_s do not show any obvious change with collision centrality, (pseudo)rapidity, and incident energy increasing. The values of σ_c increase obviously with the collision centrality and incident energy increasing, but they do not show any obvious change with the increase of the (pseudo)rapidity in central nucleus–nucleus collisions.

References

[1] Sissakian A N, Sorin A S, Suleymanov M K, Toneev V D and Zinovjev G M 2005 nucl-ex/0511018

[2] Arndt R A, Briscoe W J, Strakovsky I I and Workman R L 2006 nucl-ex/0607014

[3] Cunqueiro L, Ferreiro E G, del Moral F and Pajares C 2005 *Phys. Rev.* C **72** 024907

[4] Liu J Y, Guo W J, Ren Zh Zh, Xing Y Zh, Zuo W and Lee X G 2006 *Chin. Phys.* **15** 1738

[5] Yong G Ch, Li B A and Zuo W 2005 *Chin. Phys.* **14** 1549

[6] Zhang Y F, Huang Sh L, Zhang Z P and Wu J 2007 *Chin. Phys.* **16** 58

[7] Li Q, Jiang Zh J and Xia H F 2006 *Acta Phys. Sin.* **55** 5161 (in Chinese)

[8] Yong G Ch, Li B A, Chen L W and Zuo W 2006 *Acta Phys. Sin.* **55** 5166 (in Chinese)

[9] Bian B A, Zhou H Y and Zhang F Sh 2007 *Acta Phys. Sin.* **56** 1334 (in Chinese)

[10] Singh G, Sengupta K and Jain P L 1988 *Phys. Rev. Lett.* **61** 1073

[11] Agakichiev G, Appelshauser H, Baur R, Braun-Munzinger P, Cherlin A, Drees A, Esumi S I, Filimonov K, Fraenkel Z, Fuchs C, Glassel P, Hering G, Lenkeit B, Marn A, Messer F, Messer M, Milosevic J, Miskowiec D, Nix O, Panebratsev Y, Petracek V, Pfeiffer A, Rak J, Ravinovich I, Razin S, Rehak P, Sako H, Saveljic N, Schmitz W, Shimansky S, Socol E, Slvova J, Specht H J, Stachel J, Tilsner H, Tserruya I, Voigt C, Voloshin S, Weber C, Wessels J P, Wurm J P and Yurevich V (CERES/NA45 Collaboration) 2004 *Phys. Rev. Lett.* **92** 032301

[12] Barrette J, Bellwied R, Bennett S, Braun-Munzinger P, Cleland W E, Cormier T M, David G, Dee J, Diebold G E, Dietzsch O, Fox D, Germani J V, Gilbert S, Greene S V, Hall J R, Hemmick T K, Herrmann N, Hong B, Jayananda K, Kraus D, Kumar B S, Lacasse R, Li Q, Lissauer D, Llope W J, Ludlam T W, McCorkle S, Majka R, Mark S K, Matheus R, Mitchell J T, Muthuswamy M, O'Brien E, Panitkin S, Pruneau C, Rao M N, Rosati M, Rotondo F, da Silva N C, Simon-Gillo J, Sonnadara U, Stachel J, Sullivan J, Takai H, Takagui E M, Throwe T G, Winter C, Wang G, Wolf K L, Wolfe D, Woody C L, Xu N, Zhang Y, Zhang Z and Zou C (E814/E877 Collaboration) 1993 *Phys. Rev. Lett.* **70** 2996

[13] Jain P L, Singh G and Sengupta K 1999 *Phys. Rev.* C **43** 2027

[14] Topor Pop V, Gyulassy M, Barrette J, Gale C, Wang X N and Xu N 2004 *Phys. Rev.* C **70** 064906

[15] Broniowski W, Hiller B, Florkowski W and Bozek P 2006 *Phys. Lett.* B **635** 290

[16] Uhlig F, Forster A, Bottcher I, Debowski M, Dohrmann F, Grosse E, Koczon P, Kohlmeyer B, Laue F, Menzel M, Naumann L, Oeschler H, Scheinast W, Schwab E, Senger P, Shin Y, Strobele H, Sturm C, Surowka G, Wagner A and Walus W (KaoS Collaboration) 2005 *Phys. Rev. Lett.* **95** 012301

[17] Wang X N 1997 *Phys. Rep.* **280** 287

[18] Soff S, Randrup J, Stocker H and Xu N 2003 *Phys. Lett.* B **551** 115

[19] Bass S A, Muller B and Srivastava D K 2003 *Phys. Rev. Lett.* **91** 052302

[20] Westfall G D, Gosset J, Johansen P J, Poskanzer A M, Meyer W G, Gutbrod H H, Sandoval A and Stock R 1976 *Phys. Rev. Lett.* **37** 1202

[21] Werner K 1993 *Phys. Rep.* **232** 87

[22] Liu F H 1998 *Acta Phys. Sin. (Overseas Edition)* **7** 321

[23] Liu F H and Panebratsev Y A 1998 *Nucl. Phys.* A **641** 379

[24] Liu F H and Panebratsev Y A 1999 *Phys. Rev.* C **59** 1193

[25] Liu F H and Panebratsev Y A 1999 *Phys. Rev.* C **59** 1798

[26] Liu F H 2002 *Phys. Rev.* C **66** 047902

[27] Liu F H, Yin X Y, Tian J L and Abd Allah N N 2004 *Phys. Rev.* C **69** 034905

[28] Liu F H 2004 *Phys. Lett.* B **583** 68

[29] Liu F H 2008 *Mod. Phys. Lett.* A **23** 337

[30] Adams J, Adler C, Aggarwal M M, Ahammed Z, Amonett J, Anderson B D, Anderson M, Arkhipkin D, Averichev G S, Badyal S K, Balewski J, Barannikova O, Barnby L S, Baudot J, Bekele S, Belaga V V, Bellwied R, Berger J, Bezverkhny B I, Bhardwaj S, Bhaskar P, Bhati A K, Bichsel H, Billmeier A, Bland L C, Blyth C O, Bonner B E, Botje M, Boucham A, Brandin A, Bravar A, Cadman R V, Cai X Z, Caines H, Calderón de la Barca Sánchez M, Carroll J, Castillo J, Castro M, Cebra D, Chaloupka P, Chattopadhyay S, Chen H F, Chen Y, Chernenko S P, Cherney M, Chikanian A, Choi B, Christie W, Coffin J P, Cormier T M, Cramer J G, Crawford H J, Das D, Das S, Derevschikov A A, Didenko L, Dietel T, Dong W J, Dong X, Draper J E, Du F, Dubey A K, Dunin V B, Dunlop J C, Dutta Majumdar M R, Eckardt V, Efimov L G, Emelianov V, Engelage J, Eppley G, Erazmus B, Estienne M, Fachini P, Faine V, Faivre J, Fatemi R, Filimonov K, Filip P, Finch E, Fisyak Y, Flierl D, Foley K J, Fu J, Gagliardi C A, Gagunashvili N, Gans J, Ganti M S, Gaudichet L, Germain M, Geurts F, Ghazikhanian V, Ghosh P, Gonzalez J E, Grachov O, Grigoriev V, Gronstal S, Grosnick D, Guedon M, Guertin S M, Gupta A, Gushin E, Gutierrez T D, Hallman T J, Hardtke D, Harris J W, Heinz M, Henry T W, Heppelmann S, Herston T, Hippolyte B, Hirsch A, Hjort E, Hoffmann G W, Horsley M, Huang H Z, Huang S L, Humanic T J, Igo G, Ishihara A, Jacobs P, Jacobs W W, Janik M, Jiang H, Johnson I, Jones P G, Judd E G, Kabana S, Kaneta M, Kaplan M, Keane D, Khodyrev V Y, Kiryluk J, Kisiel A, Klay J, Klein S R, Klyachko A, Koetke D D, Kollegger T, Kopytine M, Kotchenda L, Kovalenko A D, Kramer M, Kravtsov P, Kravtsov V I, Krueger K, Kuhn C, Kulikov A I, Kumar A, Kunde G J, Kunz C L, Kutuev R K, Kuznetsov A A, Lamont M A C, Landgrat J M, Lange S, Lansdell C P, Lasiuk B, Laue F, Lauret J, Lebedev A, Lednický R, LeVine M J, Li C, Li Q, Lindenbaum S J, Lisa M A, Liu F, Liu L, Liu Z, Liu Q J, Ljubicic T, Llope W J, Long H, Longacre R S, Lopez-Noriega M, Love W A, Ludlam T, Lynn D, Ma J, Ma Y G, Magestro D, Mahajan S, Mangotra L K, Mahapatra D P, Majka R, Manweiler R, Margetis S, Markert C, Martin L, Marx J, Matis H S, Matulenko Y A, McShane T S, Meissner F, Melnick Y, Meschanin A, Messer M, Miller M L, Milosevich Z, Minaev N G, Mironov C, Mishra D, Mitchell J, Mohanty B, Molnar L, Moore C F, Mora-Corral M J, Morozov D A, Morozov V, de Moura M M, Munhoz M G, Nandi B K, Nayak S K, Nayak T K, Nelson J M, Nevski P, Nikitin V A, Nogach L V, Norman B, Nurushev S B, Odyniec G, Ogawa A, Okorokov V, Oldenburg M, Olson D, Paic G, Pandey S U, Pal S K, Panebratsev Y, Panitkin S Y, Pavlinov A I, Pawlak T, Perevoztchikov V, Perkins C, Peryt W, Petrov V A, Phatak S C, Picha R, Planinc M, Pluta J, Porile N, Porter J, Poskanzer A M, Potekhin M,

Potrebenikova E, Potukuchi B V K S, Prindle D, Pruneau C, Putschke J, Rai G, Rakness G, Raniwala R, Raniwala S, Ravel O, Ray R L, Razin S V, Reichhold D, Reid J G, Renault G, Retiere F, Ridiger A, Ritter H G, Roberts J B, Rogachevski O V, Romero J L, Rose A, Roy C, Ruan L J, Sahoo R, Sakrejda I, Salur S, Sandweiss J, Savin I, Schambach J, Scharenberg R P, Schmitz N, Schroeder L S, Schweda K, Seger J, Seliverstov D, Seyboth P, Shahaliev E, Shao M, Sharma M, Shestermanov K E, Shimanskii S S, Singaraju R N, Simon F, Skoro G, Smirnov N, Snellings R, Sood G, Sorensen P, Sowinski J, Spinka H M, Srivastava B, Stanislaus S, Stock R, Stolpovsky A, Strikhanov M, Stringfellow B, Struck C, Suaide A A P, Sugarbaker E, Suire C, Šumbera M, Surrow B, Symons T J M, Szanto de Toledo A, Szarwas P, Tai A, Takahashi J, Tang A H, Thein D, Thomas J H, Tikhomirov V, Tokarev M, Tonjes M B, Trainor T A, Trentalange S, Tribble R E, Trivedi M D, Trofimov V, Tsai O, Ullrich T, Underwood D G, Van Buren G, VanderMolen A M, Vasiliev A N, Vasiliev M, Vigdor S E, Viyogi Y P, Voloshin S A, Waggoner W, Wang F, Wang G, Wang X L, Wang Z M, Ward H, Watson J W, Wells R, Westfall G D, Whitten C, Wieman H, Willson R, Wissink S W, Witt R, Wood J, Wu J, Xu N, Xu Z, Xu Z Z, Yamamoto E, Yepes P, Yurevich V I, Zanevski Y V, Zborovský I, Zhang H, Zhang W M, Zhang Z P, Żolnierczuk P A, Zoulkarneev R, Zoulkarneeva J and Zubarev A N (STAR Collaboration) 2003 nucl-ex/0311017.

[31] Klay J L, Ajitanand N N, Alexander J M, Anderson M G, Best D, Brady F P, Case T, Caskey W, Cebra D, Chance J L, Chung P, Cole B, Crowe K, Das A C, Draper J E, Gilkes M L, Gushue S, Heffner M, Hirsch A S, Hjort E L, Huo L, Justice M, Kaplan M, Keane D, Kintner J C, Krofcheck D, Lacey R A, Lauret J, Law C, Lisa M A, Liu H, Liu Y M, McGrath R, Milosevich Z, Odyniec G, Olson D L, Panitkin S Y, Pinkenburg C, Porile N T, Rai G, Ritter H G, Romero J L, Scharenberg R, Srivastava B, Stone N T B, Symons T J M, Wang S, Wells R, Whitfield J, Wienold T, Witt R, Wood1 L and Zhang W N (E895 Collaboration) 2003 *Phys. Rev.* C **68** 054905